A SELF-ADAPTING TARGET STATE ESTIMATOR

ROBERT A. SCHEDER
USA MATERIEL SYSTEMS ANALYSIS ACTIVITY
ABERDEEN PROVING GROUND, MD 21005

1. INTRODUCTION

Determining a target aircraft's position, velocity, and acceleration from measurement of its position is a major problem in modern antiaircraft gun, laser, and missile fire control. (References 1 and 2). Many versions of the optimal or Kalman state estimator have been used with varying degrees of success. (References 3, 4, and 5). This paper offers a new technique which allows detailed aircraft flight dynamics and constraints to be incorporated into the general Kalman structure.

The Kalman estimator is viewed as a set of algorithms that uses sensor (e.g., radar) data, the statistical properties of the sensor errors, the equations of the target motion, and the statistical properties of the errors of these equations to produce estimates of target position, velocity, and acceleration.

Let X denote the target's state 9 vector. The discretized dynamical equation is:

$$X(n+1) = \Phi(n)\, X(n) + N(n), \qquad (1.0)$$

where n denotes the time step. The state transition or plant 9 X 9 matrix, $\Phi(n)$, embodies target dynamics. The plant noise random 9 vector, N(n), accounts for both the aircraft dynamics neglected by the plant and the randomness of pilot commands.

Let E denote expected value and superscript T denote transpose. The n^{th} target state estimate, $\hat{X}(n)$, and the corresponding state error covariance matrix, $P(n) = E(X(n) - \hat{X}(n))(X(n) - \hat{X}(n))^T$, are extrapolated to time step n+1 by means of equation 1.0. The extrapolations are corrected by the sensor measurement 3 vector Z(n+1) received at time step n+1.

The extrapolation stage consists of equations 1.1 and 1.2 below,

$$X^e(n) = \Phi(n)\ \hat{X}(n) + \bar{N}(n) \qquad (1.1)$$

where superscript e denotes extrapolated value and $(\bar{})$ denotes most probable value. The extrapolated state error covariance $P^e(n)$, is defined as,

$$E(X(n+1) - X^e(n))(X(n+1) - X^e(n))^T.$$

This definition, equation 1.1, and the assumption

$$E(X(n) - \hat{X}(n))\ (N(n) - \bar{N}(n)^T = 0 \quad \text{yields:}$$

$$P^e(n) = \Phi(n)\ P(n)\ \Phi^T(n) + Q(n), \qquad (1.2)$$

where the plant noise covariance 9 X 9 matrix Q(n), is defined as:

$$Q(n) = E(N(n) - \bar{N}(n))(N(n) - \bar{N}(n))^T.$$

At time step n+1, a new sensor measurement is received,

$$Z(n+1) = H(n+1)\ X(n+1) + V(n+1).$$

The state to measurement transformation 3 X 9 matrix, H(n+1), relates the state vector to the measurement vector (measurement-state combinations are discussed in Reference 6). The zero mean random sensor error is V(n+1) (e.g., thermal noise).

The estimator weighs the confidence in the measurement Z(n+1) against the confidence in the extrapolated state $X^e(n)$ and distributes the 3 vector difference, Z(n+1) - H(n+1) X(n), to correct appropriately the extrapolated state 9 vector, $X^e(n)$. Consider,

$$J = (\hat{X}(n+1) - X^e(n))\ P^{e-1}_{(n)}\ (\hat{X}(n+1) - X^e(n))^T + (Z(n+1) - H(n+1)\ \hat{X}(n+1))\ R^{-1}(n+1)\ (Z(n+1) - H(n+1)\ \hat{X}(n+1))^T$$

where R(n+1), the measurement noise covariance matrix, equals

$$E\ V(n+1)\ V(n+1)^T.$$

Choosing $\hat{X}(n+1)$ to minimize J has the desirable effect of forcing $\hat{X}(n+1)$ close to $X^e(n)$ when $P^e(n)$ is small (i.e., high confidence in $X^e(n)$) and forcing H(n+1) X(n+1) close to Z when R(n+1) is small (i.e., high confidence in Z). Setting the derivative of J to zero yields:

$$\hat{X}(n+1) = X^e(n) + K(n)\ (Z(n+1) - H(n+1)\ X^e(n)) \qquad (1.3)$$

where the Kalman gain 9 X 3 matrix K(n) is given by:

$$K(n) = P^e(n)\ H^T(n+1)\ (H(n+1)\ P^e(n)\ H^T(n+1) + R(n+1))^{-1} \qquad (1.4)$$

The state error covariance matrix at the n+1 time step,

$$P(n+1) = E(X(n+1) - \hat{X}(n+1))\ (X(n+1) - \hat{X}(n+1))^T,$$

computed with the assumption $E(X(n+1) - X^e(n))V^T(n) = 0$ yields:

$$P(n+1) = P^e(n) - K(n)\ H(n+1)\ P^e(n). \qquad (1.5)$$

Equations 1.1 through 1.5, recognized as the Kalman algorithms (Reference 7), may be used iteratively to compute $\hat{X}$ for all n.

2. DEVELOPMENT OF Φ, Q AND $\bar{N}$

Once the algorithms have been initialized, Φ, R, Q, H, and $\bar{N}$ can be updated to incorporate information generated from past state estimates. Nonlinear processes always require this sort of self-adapting mechanism. Adaptive bandwidth, hypothesis testing, and residual testing filters are further examples that use past state estimates (Reference 8).

Two self-adapting methods which incorporate detailed target dynamics and constraints into Φ, Q, and $\bar{N}$ are developed below.

2.1 The Plant Noise Mean Method.

Express the target state in earth coordinates and choose a plant matrix, Φ, that represents the dynamics of an aircraft whose Cartesian earth frame acceleration is constant over a time step.

$$\Phi = \begin{bmatrix} I_{3x3} & dt\ I_{3x3} & \frac{dt^2}{2}\ I_{3x3} \\ 0_{3x3} & I_{3x3} & dt\ I_{3x3} \\ 0_{3x3} & 0_{3x3} & I_{3x3} \end{bmatrix}$$

where dt is the time step length, and I is the identity 3x3 matrix. The plant noise vector then takes the form,

$$N = \begin{bmatrix} \frac{dt^3}{6}\dot{A}_3 \\ \frac{dt^2}{2}\dot{A}_3 \\ dt\dot{A}_3 \end{bmatrix} \quad , \quad \bar{N} = \begin{bmatrix} \frac{dt^3}{6}\bar{\dot{A}}_3 \\ \frac{dt^2}{2}\bar{\dot{A}}_3 \\ dt\bar{\dot{A}}_3 \end{bmatrix}$$

$$Q = \begin{bmatrix} \frac{dt^6}{36} & \frac{dt^5}{12} & \frac{dt^4}{6} \\ \frac{dt^5}{12} & \frac{dt^4}{4} & \frac{dt^3}{2} \\ \frac{dt^4}{6} & \frac{dt^3}{2} & dt^2 \end{bmatrix} Q'_{3x3}$$

where $\dot{A}$ is the target's earth frame acceleration rate 3 vector and Q' is the target's earth frame acceleration rate covariance 3x3 matrix. The above formulation is essentially a Taylor expansion of the target's position vector. The plant, Φ, accounts for the zero, first, and second derivatives while the plant noise, N, is the remainder term. N is thus identified with the target's acceleration rate.

The acceleration rate statistics are controlled both by the desires of the pilot and the maneuver capabilities of the aircraft. For example, the greater the target's capability to change the number of g's that it's pulling, the poorer the constant acceleration

assumption becomes (i.e., the poorer the plant ϕ) and the larger the acceleration rate variance. The following analysis translates physical properties in aircraft body coordinates to mathematical properties in the earth reference frame. For clarity, a zero gravitational field is considered first and the results then extended to the more realistic 1g field.

At any particular instant, a circle can be fitted to the target's flight path so that the target velocity vector is tangent to its circumference and that the component of target acceleration perpendicular to the velocity vector points towards its center (Reference 9). The target acceleration is then expressed as,

$$A = \dot{V}1_V + kV^2 1_N \tag{2.1}$$

where V equals the magnitude of the target velocity, 1_V is the unit vector in the direction of target velocity, and 1_N is the principal normal. 1_N, which is perpendicular to the target velocity vector and points toward the center of curvature, equals $(kV)^{-1}\dot{1}_V$. The curvature, k, is given by $|V1_V \text{ cross } A|V^{-3}$ ($1/k$ = radius curvature).

In this coordinate frame, a simple relationship exists between target acceleration and physical aircraft quantities. The force on the target can be expressed as,

$$F = T1_V + AP1_N \tag{2.2}$$

where: F = force per unit mass vector,
T = net thrust per unit mass, and
AP = air pressure force per unit mass.

Comparing equations 2.1 and 2.2,

$$\begin{aligned} T &= \dot{V} \\ AP &= kV^2 \end{aligned} \tag{2.3}$$

A simple relationship also exists between acceleration rate and the pilot controlled physical quantities of thrust rate, roll rate, and g rate. Differentiating equation 2.1,

$$\dot{A} = \dot{T}1_V + T\dot{1}_V + \dot{AP}1_N + AP\dot{1}_N \tag{2.4}$$

and noting the Frenet equations (Reference 9),

$$\begin{aligned} \dot{l}_V &= kVl_N \\ \dot{l}_N &= -kVl_V + \tau Vl_B \\ \dot{l}_B &= -\tau Vl_N \end{aligned} \tag{2.5}$$

where τ is the torsion, $\tau V = W$ = target roll rate, and $l_B = l_V$ cross l_N, and resolving $\dot{A}$ along the Frenet axis, yield:

$$\begin{aligned} \dot{A} \text{ dot } l_V &= \dot{T} - k^2V^3 \\ \dot{A} \text{ dot } l_N &= kV\dot{V} + \dot{AP} \\ \dot{A} \text{ dot } l_B &= kV^2W \end{aligned} \tag{2.6}$$

$\dot{T}$, $\dot{AP}$, and W are pilot controlled and are modeled as zero mean random variables. Therefore, in the reference earth coordinate frame,

$$\bar{\dot{A}} = T_{FR} \begin{pmatrix} -k^2V^3 \\ kV\dot{V} \\ 0 \end{pmatrix} \tag{2.7a}$$

$$Q' = T_{FR}\, Q'_F\, T_{FR}^T$$

$$Q'_F = \begin{pmatrix} E\,\dot{T}^2 & 0.0 & 0.0 \\ 0.0 & E\,\dot{AP}^2 & 0.0 \\ 0.0 & 0.0 & kV^2EW^2 \end{pmatrix} \tag{2.7b}$$

where $\bar{\dot{A}}$ is recognized as the most probable value of the acceleration rate in reference coordinates, and Q' as the target's earth frame acceleration rate covariance. T_{FR} is the Frenet frame to reference frame coordiante transformation and Q'_F the acceleration rate covariance in Frenet coordinates. The random variables $\dot{T}$, $\dot{AP}$, and W are assumed independent.

N, $\bar{N}$, and Q are computed in terms of V, k, T_{RF}, $E(\dot{T}^2)$, $E(\dot{AP}^2)$, and $E\,W^2$. V, k, and T_{RF} are computed each time step in terms of the most recent state estimate ($T_{RF} = T_{FR}^T$),

$$V = (\hat{X}_4^2 + \hat{X}_5^2 + \hat{X}_6^2)^{1/2}$$

$$\dot{V} = (\hat{X}_4 \hat{X}_7 + \hat{X}_5 \hat{X}_8 + \hat{X}_6 \hat{X}_9)/V$$

$$k = ((\hat{X}_5 \hat{X}_9 - \hat{X}_6 \hat{X}_8)^2 + (\hat{X}_4 \hat{X}_9 - \hat{X}_7 \hat{X}_6)^2 + (\hat{X}_4 \hat{X}_8 - \hat{X}_5 \hat{X}_7)^2)^{1/2}/V^3$$

$$T_{RF}^{11} = \hat{X}_4/V \qquad T_{RF}^{21} = (\hat{X}_7 - \hat{X}_4 A_T)/G_N$$

$$T_{RF}^{12} = \hat{X}_5/V \qquad T_{RF}^{22} = (\hat{X}_8 - \hat{X}_5 A_T)/G_N$$

$$T_{RF}^{13} = \hat{X}_6/V \qquad T_{RF}^{23} = (\hat{X}_9 - \hat{X}_6 A_T)/G_N$$

$$T_{RF}^{31} = T_{RF}^{12} T_{RF}^{23} - T_{RF}^{13} T_{RF}^{22}$$

$$T_{RF}^{32} = T_{RF}^{21} T_{RF}^{13} - T_{RF}^{11} T_{RF}^{23}$$

$$T_{RF}^{33} = T_{RF}^{11} T_{RF}^{22} - T_{RF}^{21} T_{RF}^{12} \qquad (2.8)$$

where $A_T = (\hat{X}_4 \hat{X}_7 + \hat{X}_5 \hat{X}_8 + \hat{X}_6 \hat{X}_9)/V^2$ and $G_N = kV^2$. Typical maximum aircraft rates are given in Table 2-1. Values used during validation of the method are also given.

TABLE 2.1 AIRCRAFT ACCELERATION RATE

Maximum Rates		Mechanized Values (One Standard Deviation)
$\dot{T}$ (M/sec^3)	10.0	3.5
$\dot{AP}$ (M/sec^3)	20.0	7.0
W (rad/sec)	3.2	1.1

Extending this idea to a gravitational field requires distribution of gl_Z to the Frenet axes.

$$T = \dot{V} + gl_Z dotl_V$$

$$AP = [g^2(l_Z dotl_B)^2 + (gl_Z dotl_N + kV^2)^2]^{\frac{1}{2}} \qquad (2.9)$$

where: T = target thrust minus drag, and
AP = aerodynamic force perpendicular to the target's wings, and $-gl_Z$ is the grativational acceleration vector.

Equation 2.9 implies:

$$\ddot{V} = \dot{T} - gkVl_Z dotl_N$$

$$(k\dot{V}^2) = c_1\dot{AP} + c_2 W + gkVl_2 dotl_V$$

where: $c_1 = AP/(gl_Z dotl_N + kV^2)$

$$c_2 = -gkV^2 l_Z dotl_B/(gl_Z dotl_N + kV^2).$$

Equation 2.6 becomes:

$$\dot{A}dotl_V = \dot{T} - gkVl_Z dotl_N - k^2V^3$$

$$\dot{A}dotl_N = kV\dot{V} + gkVl_Z dotl_V + c_1\dot{AP} + c_2 W$$

$$\dot{A}dotl_B = kV^2 W \qquad (2.10)$$

Hence, analogus to equation 2.7:

$$\dot{\bar{A}} = T_{FR} \begin{pmatrix} -gkV\, l_Z dotl_N - k^2V^3 \\ kV\dot{V} + gkV\, l_Z dotl_V \\ 0.0 \end{pmatrix}$$

$$Q'_F = \begin{pmatrix} E\dot{T}^2 & 0.0 & 0.0 \\ 0.0 & c_1^2 E\dot{AP}^2 + c_2^2 EW^2 & c_2 kV^2 EW^2 \\ 0.0 & c_2 kV^2 EW^2 & k^2V^4 EW^2 \end{pmatrix}$$

2.2 The Dynamical Plant Method.

The acceleration rate mean can readily be incorporated into the plant matrix Φ. Let A_F equal the acceleration vector in the Frenet frame, then,

$$A_R = T_{FR}\, A_F$$

$$\dot{A}_R = T_{FR}\, \dot{A}_F + \dot{T}_{FR}\, A_F$$

which can be written:

$$\dot{A}_R = T_{FR}\, (T_{FR}^T\, \dot{T}_{FR})\, T_{FR}^T\, A_R + T_{FR}\, \dot{A}_F$$

where:

$$T_{FR}^T \dot{T}_{FR} = \begin{pmatrix} 0 & -kV & 0 \\ kV & 0 & -W \\ 0 & W & 0 \end{pmatrix}$$

$$\dot{A}_F = \begin{pmatrix} \dot{T} \\ \dot{AP} \\ 0 \end{pmatrix}$$

Therefore,

$$\dot{A}_R = T_{FR} \begin{pmatrix} 0 & -kV & 0 \\ kV & 0 & 0 \\ 0 & 0 & 0 \end{pmatrix} T_{FR}^T\, A_R + T_{FR} \begin{pmatrix} \dot{T} \\ \dot{AP} \\ kV^2W \end{pmatrix} \qquad (2.11)$$

is the desired zero mean plant noise formulation. For example, consider an aircraft flying in a deterministic circle, then, its X and Y components of acceleration satisfy:

$$A_X = G \cos \omega t$$

$$A_Y = G \sin \omega t$$

$$\dot{A}_X = -\omega\, G \sin \omega t$$

$$\dot{A}_Y = \omega\, G \cos \omega t \qquad (2.12)$$

where $R = 1/k$ is the radius of the flight path circle, $\omega = V/R$, and $G = |A|$. Equation 2.12 can be written as a special case of equation 2.11.

$$\begin{pmatrix} \dot{\Lambda}_X \\ \dot{\Lambda}_Y \end{pmatrix} = \begin{pmatrix} 0 & -kV \\ kV & 0 \end{pmatrix} \begin{pmatrix} \Lambda_X \\ \Lambda_Y \end{pmatrix}$$

The example also illustrates the essential equivalence of the two methods. Since $\dot{T} = \dot{AP} = W = \dot{V} = 0$ and $k^2V^3 = G\omega$, equations 2.7a and 2.8 imply,

$$\dot{A} = T_{FR} \begin{pmatrix} -G\omega \\ 0 \\ 0 \end{pmatrix}$$

$$T_{FR} = \begin{pmatrix} \sin \omega t & \cos \omega t & 0 \\ -\cos \omega t & \sin \omega t & 0 \\ 0 & 0 & 1 \end{pmatrix} .$$

Therefore,

$$\dot{A} = \begin{pmatrix} -G\omega \sin \omega t \\ G\omega \cos \omega t \\ 0 \end{pmatrix}$$

which is consistant with equation 2.12.

Both methods essentially color the target's acceleration by fitting the instantaneous Frenet circle to the latest estimated target state. With proper account given to the gravitational field, this expresses the plant noise in the target related quantities $\dot{T}$, $\dot{AP}$, and W.

3. CONCLUSIONS

Through the use of the Frenet equations, target roll rate, thrust rate, and g rate are embedded into the estimator formulation. This enables the estimator to provide more accurate state error covariances resulting in improved state estimates. Similarly, incorporating the deterministic portion of the target's acceleration rate, $\dot{\bar{N}}$, provides a further improvement, particularly helpful along coordinated target turns.

Computer simulations were used to compare the plant noise mean estimator to a close copy of the Gun Low Altitude Air Defense

System (GLAADS) estimator (Reference 4). The GLAADS estimator was chosen for reference because it performed very successfully during the recent field tests. It takes excellent advantage of modern analytical techniques and most importantly it is formulated similar to the plant noise mean estimator. The principal difference is that the GLAADS estimator lacks an $\bar{N}$ term and uses a simpler plant error covariance. The differences in performance are quantified in Figure 3.1 which compares the magnitude of the acceleration errors of the two estimators for an aircraft in a 4g coordinated turn. After a 2-3 second settling time, the advantage of including detailed target dynamics is apparent.

Additional benefits arise naturally from the physical approach taken by the plant noise mean and dynamical plant methods. For example, Table 3.1 compares prediction accuracy obtained by iterating equation 1.1 with and without the $\bar{N}$ term. Including $\bar{N}$ results in prediction along the Frenet circle while omitting its results in constant acceleration extrapolation. The two predictors are compared for various prediction times (e.g., bullet times of flight) along various coordinated turns. The table indicates that the relative superiority of the Frenet circle predictor grows with target g's and prediction times. In general, it is at least as good as the constant acceleration extrapolator along noncoordinated maneuvers.

These ideas can be practically applied to real systems. The estimator-predictor algorithms, equations 1.1 through 1.5, slightly modified to include the singular case, K=0, have proven to be completely stable for circular, popup and dive, straight line and jinking target trajectories. The engineering expertise required to construct the appropriate hardware has already been successfully demonstrated in the GLAADS program. In fact, the improved estimator-predictor could easily be programmed into the present GLAADS computer.

In conclusion, the plant noise mean and the dynamical plant methods provide improvements to current state estimation technology and offer an approach to incorporating real target constraints into fire control logic. In terms of practical payoff, these methods will enable the proposed Army Radar Gun Air Defense System (ARGADS) to more successfully engage maneuvering targets.

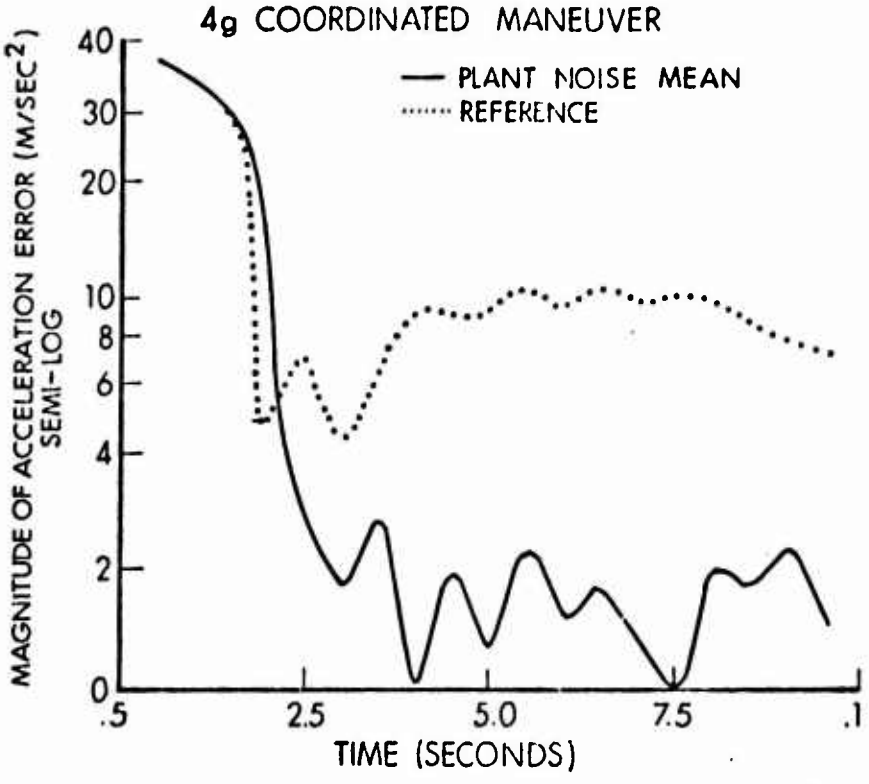

Figure 3.1. Comparison of Estimator Accuracy.

FRENET CIRCLE/CONSTANT ACCELERATION

SEC/G'S	1	2	3	4
1	0.0/0.1	0.0/0.2	0.0/0.5	0.0/0.9
2	0.0/0.4	0.0/1.8	0.0/4.0	0.0/7.1
3	0.0/1.5	0.0/6.0	0.1/13.5	0.2/23.9
4	0.0/3.6	0.0/14.2	0.2/31.9	0.4/56.6

MAGNITUDE OF PREDICTED POSITION ERROR (METERS)

TABLE 3.1 COMPARISON OF PREDICTOR ACCURACY

REFERENCES

1. Burke, H.H., and Perkins, T.R., Anti-Aircraft Gun Fire Control System Status, Evaluation Methodology, and Simulation, US Army Materiel Systems Analysis Activity, Combat Support Division, Aberdeen Proving Ground, MD (To be published).

2. Scheder, R.A., Modern Fire Control Analysis, Second Annual Automatic Cannon Caliber Munitions Symposium, Frankford Arsenal, Philadelphia, PA, 1976.

3. Singer, R.A., and Behnke, K.W., Real-Time Tracking Filter Evaluations and Selection for Tactical Applications, IEEE Transactions on Aero and Electronic Systems, Volume AES-7 No. 1, January 1971, (p #100).

4. McCarthy, J.R., and Villalabos, G.D., Gun Low Altitude Air Defense System (GLAADS) Mechanization, Autonetics Group Rockwell International, Anaheim, CA, 1974.

5. Rivoire, J.M., Precision Tracking, Applied Physics Lab - Johns Hopkins University (TG 1237), Silver Spring, MD, 1974.

6. Leathrum, James F., An Approach to Fire Control System Computations and Simulations, US Army Materiel Systems Analysis Activity, Aberdeen Proving Ground, MD, 1975.

7. Bryson, A.E., Jr., and Ho, Yu-Chi, Applied Optimal Control, Ginn and Company, Waltham, MA, 1969.

8. Brown, C.M., Jr., and Price, C.F., Adaptive Tracking Filter Design and Evaluation for Gun Fire Control Systems, The Analytical Science Corporation, Reading, MA, 1974.

9. Stoker, J.J., Differential Geometry, Wiley-Interscience, New York, NY, 1969.